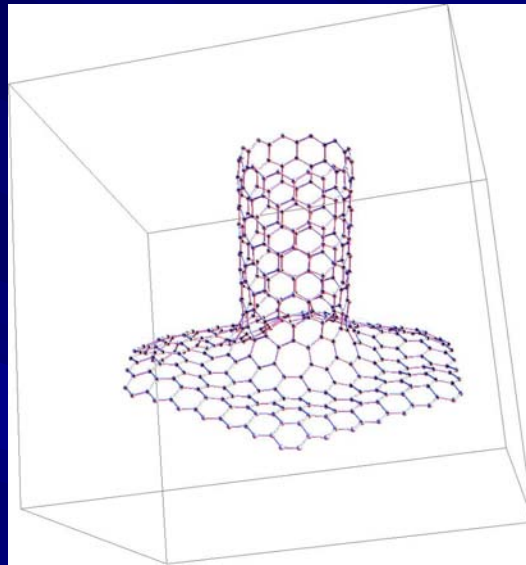


# CARBON NANOTUBE-GRAPHENE JUNCTIONS



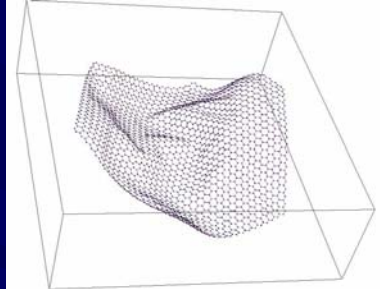
J. González

Instituto de Estructura de la Materia, CSIC, Spain

(work in collaboration with F. Guinea and J. Herrero)

# CURVATURE IN GRAPHENE

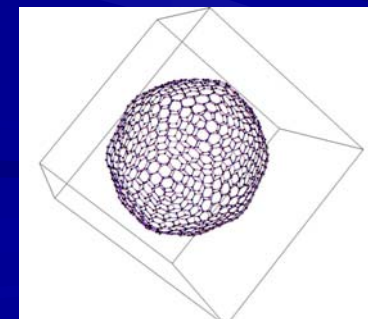
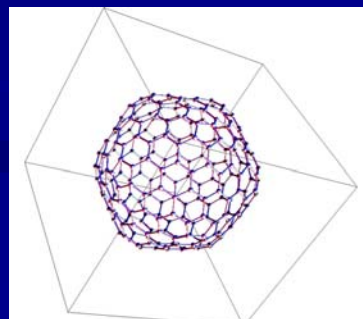
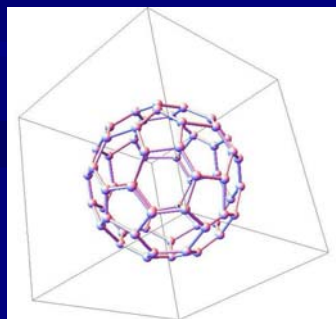
## ■ CURVATURE:



The effects of curvature are important in graphene, as the existence of ripples in the carbon layer is an intrinsic feature, that may be influencing important properties in the electronic transport.

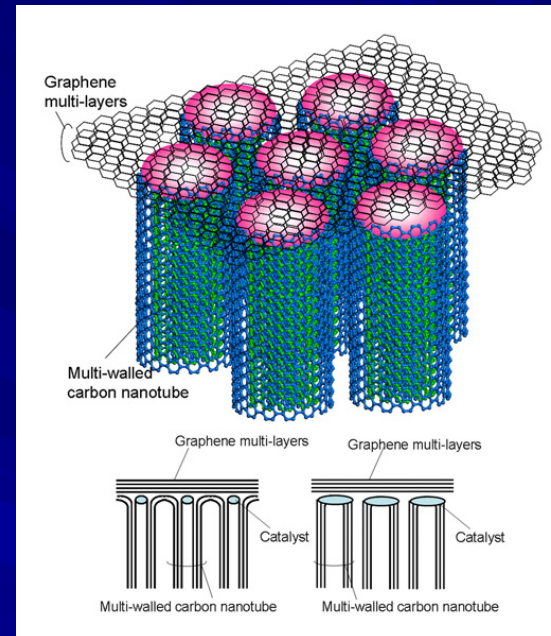
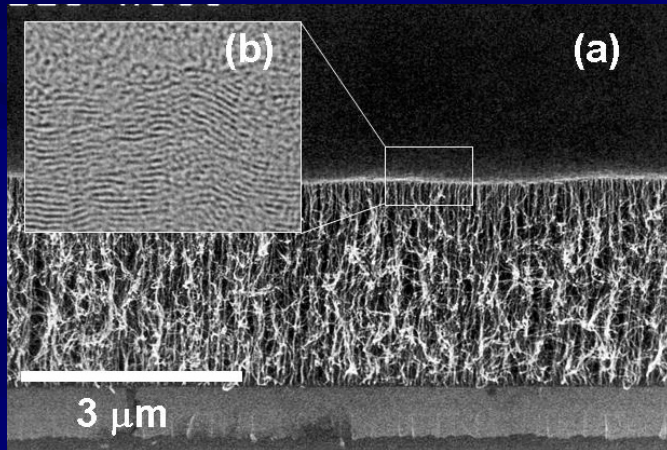
## ■ CURVATURE + TOPOLOGY:

In this talk we are going to discuss the kind of curvature that induces changes in the topology of the carbon material. The case of the fullerenes is the best known example



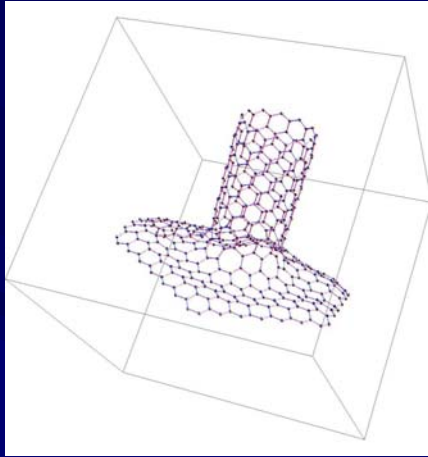
# CURVATURE IN GRAPHENE

It seems that carbon nanotube-graphene junctions have been already fabricated in the Fujitsu Laboratories



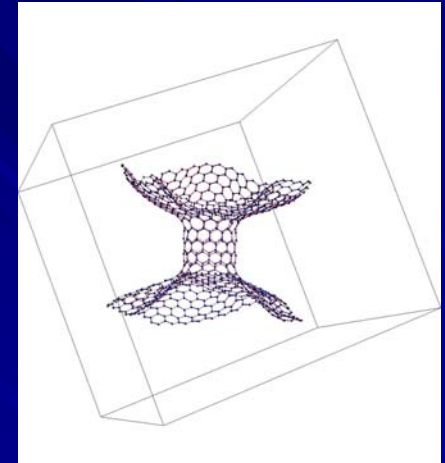
(from Fujitsu Laboratories Ltd.)

## CURVATURE IN GRAPHENE



Can we learn something from the effect of negative curvature in the carbon layer?

Again, the induced change of topology requires topological defects, and these may give rise to interesting features in the electronic structure.



# TOPOLOGY OF GRAPHENE SHEETS

2D geometries can be classified according to the values of the Euler characteristic

$$\chi = \frac{1}{4\pi} \int d^2x \sqrt{g} R$$

This is in general an integer number, that only depends on the topology of the surface.

It can be also expressed for a lattice as  $\chi = \# \text{vertices} - \# \text{edges} + \# \text{faces}$

We can compute the contribution of a hexagon to  $\chi$  as

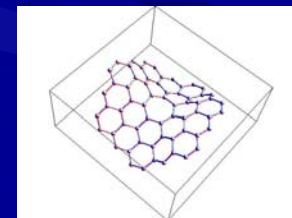
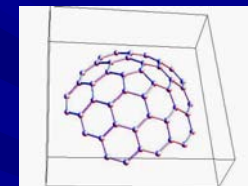
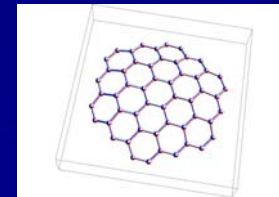
$$\Delta\chi = 2 - 3 + 1 = 0 \quad ,$$

the contribution of a pentagon as

$$\Delta\chi = \frac{5}{3} - \frac{5}{2} + 1 = \frac{1}{6} \quad ,$$

and the contribution of a heptagon as

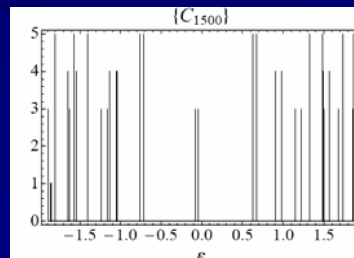
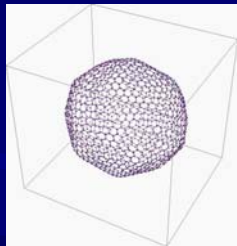
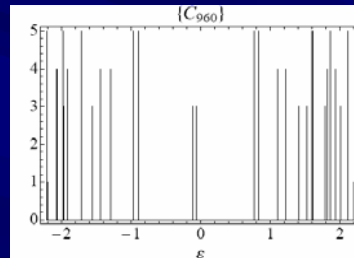
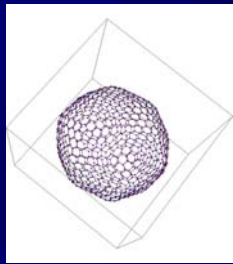
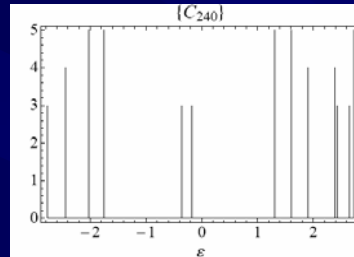
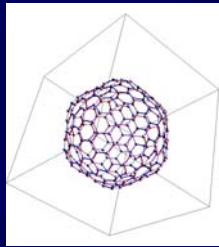
$$\Delta\chi = \frac{7}{3} - \frac{7}{2} + 1 = -\frac{1}{6}$$



This is why 12 pentagons are only needed to close the carbon lattice into a spherical shape, provided that their effect is not counterbalanced by the negative curvature of the heptagons.

# TOPOLOGY OF GRAPHENE SHEETS

While the number of defects needed to change the topology of the carbon lattice is small and always the same (12), they induce a strong effect in the electronic properties of the material



The electronic spectra of the series of very large fullerenes are remarkable, as one recovers the degeneracy of the multiplets of the angular momentum (3, 5, 7, ...), but  $l=1$  turns out to be the lowest possible value.

Moreover, if the rotational symmetry is realized approximately for very large fullerenes, it seems that the Dirac equation on the surface of a sphere

$$i\gamma \cdot \nabla \Psi_n = \varepsilon_n \Psi_n$$

should give a sensible description of the spectrum. However, it is well-known that the equation on the curved space does not have zero modes,

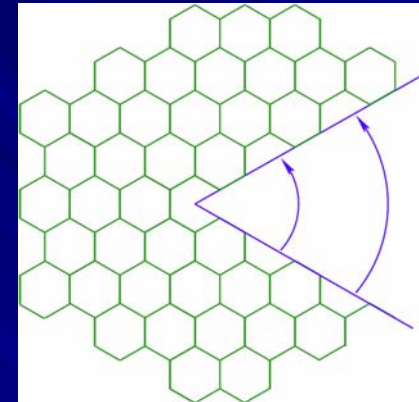
$$\varepsilon_j = \pm \left( j + \frac{1}{2} \right) \frac{1}{R}$$

J. G., F. Guinea and M.A.H. Vozmediano,  
Nucl. Phys. B 406, 771 (1993)

# TOPOLOGICAL DEFECTS IN GRAPHENE

The pentagonal carbon rings can be formed by a cut and paste operation in the plane. This induces an effective rotation of  $\pi/3$  at the junction, which implies in turn the exchange of the two Dirac valleys

$$\begin{pmatrix} \Psi'_{K'} \\ \Psi'_{K} \end{pmatrix} = \begin{pmatrix} 0 & 1 \\ -1 & 0 \end{pmatrix} \begin{pmatrix} \Psi_K \\ \Psi_{K'} \end{pmatrix}$$

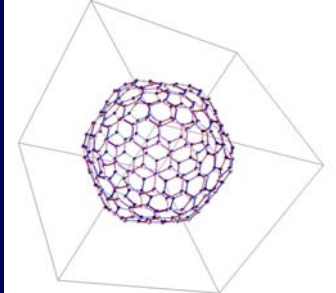


The exchange of the two Dirac valleys is only felt when making a complete turn around the topological defect. Therefore, the effect can be mimicked by a line of effective gauge flux  $\Phi$  threading the pentagonal ring, acting on the  $(K, K')$  space

$$A_\phi = \frac{\Phi}{2\pi} \begin{pmatrix} 0 & -i \\ i & 0 \end{pmatrix}$$

$$\exp\left(i \oint d\phi A_\phi\right) = \begin{pmatrix} 0 & 1 \\ -1 & 0 \end{pmatrix} \Leftrightarrow \Phi = \frac{\pi}{2}$$

## TOPOLOGICAL DEFECTS IN GRAPHENE



In the fullerenes, the combined effect of the 12 pentagonal rings is consistent with the field of a monopole, whose charge is dictated by the total flux

$$g = \frac{1}{4\pi} \sum_{i=1}^{12} \frac{\pi}{2} = \frac{3}{2}$$

By approximating the effective gauge field by an isotropic flux at the spherical surface of the fullerene, the Dirac equation for the curved lattice becomes

$$i\boldsymbol{\gamma} \cdot (\nabla - i\mathbf{A}) \Psi_n = \varepsilon_n \Psi_n$$

where  $\mathbf{A}$  is the effective gauge field mixing the spinors at  $K$  and  $K'$ .

The problem can be solved by passing to the operators  $\mathbf{J}$  of the total angular momentum operator for the spinors, curvature and gauge field, which leads to the equation

$$\left( \mathbf{J}^2 + \frac{1}{4} - g^2 \right) \Psi_n = \varepsilon_n^2 R^2 \Psi_n$$

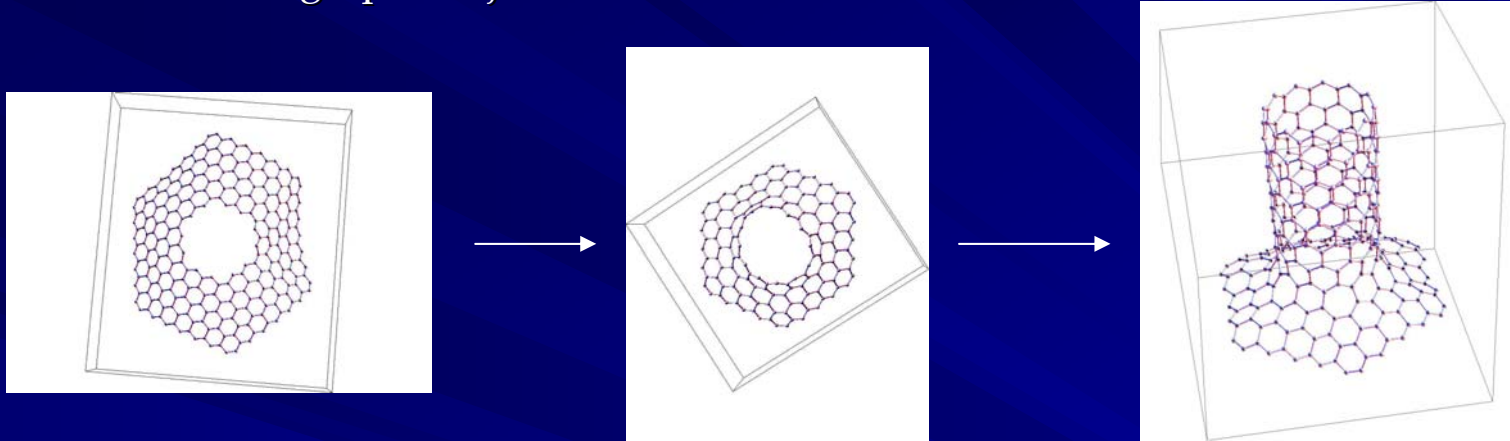
The spectrum is then given in terms of the angular momentum number  $j$

$$\varepsilon_j^2 R^2 = \left( j + \frac{1}{2} \right)^2 - g^2$$

which, for  $g = 3/2$ , accounts for the existence of two triplets of zero modes with  $j = 1$ .

# CARBON NANOTUBE-GRAPHENE JUNCTIONS

We can also investigate the effects of negative curvature in graphene. The simplest instance is a carbon nanotube-graphene junction



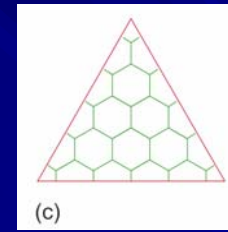
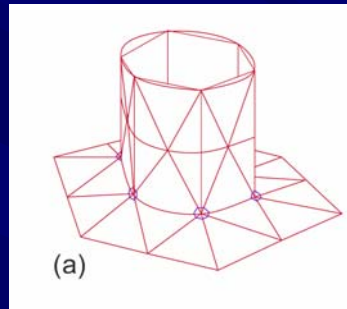
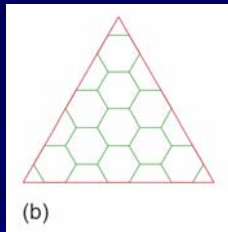
The nanotube-graphene junction requires an amount of negative curvature corresponding to 6 heptagons. This is consistent with the fact that, in any continuum geometry matching the plane with a tube, we find the Euler characteristic

$$\chi = \frac{1}{4\pi} \int d^2x \sqrt{g} R = -1$$

The above procedure describes the construction of junctions with zig-zag nanotubes of type  $(6n,0)$ . When the heptagons are regularly distributed, these are the only possible geometries, together with the junctions made of armchair  $(6n,6n)$  nanotubes.

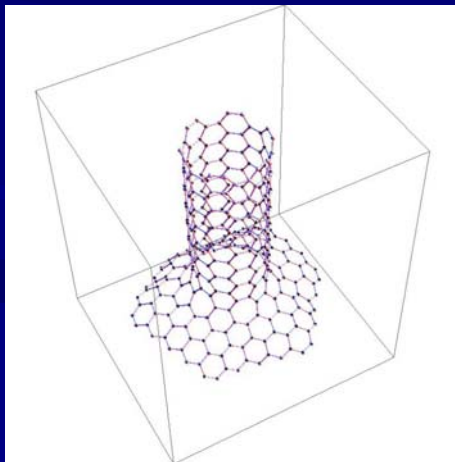
# CARBON NANOTUBE-GRAPHENE JUNCTIONS

There is a general, compact way of describing the nanotube-graphene junctions, when the topological defects (heptagons) are regularly distributed. We can think of all possible geometries as assemblies of triangular blocks of honeycomb lattice

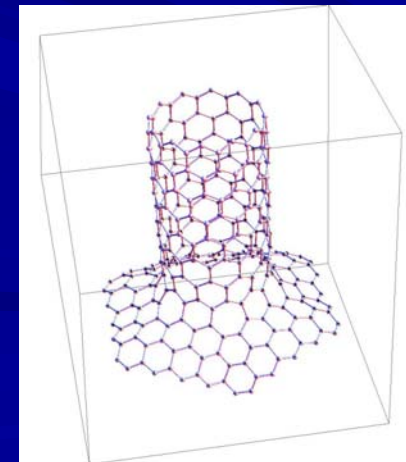


This shows again that the number of heptagonal carbon rings is always the same (6). It also becomes clear that junctions with armchair nanotubes are possible, with geometries  $(6n,6n)$ .

$(6n,6n)$



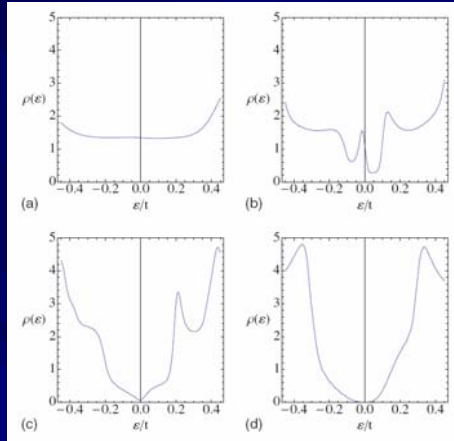
$(6n,0)$



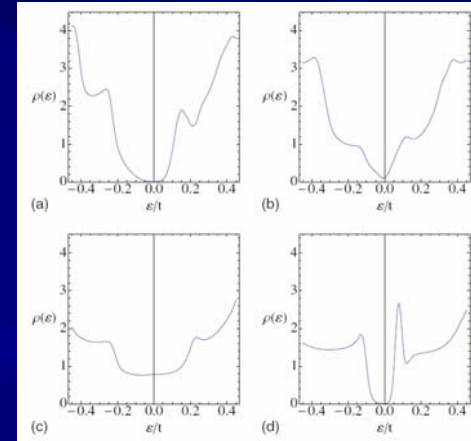
# CARBON NANOTUBE-GRAPHENE JUNCTIONS

Now we may ask about the electronic properties of these nanotube-graphene junctions. The most interesting features appear in the local density of states close to the junction

(54,0)



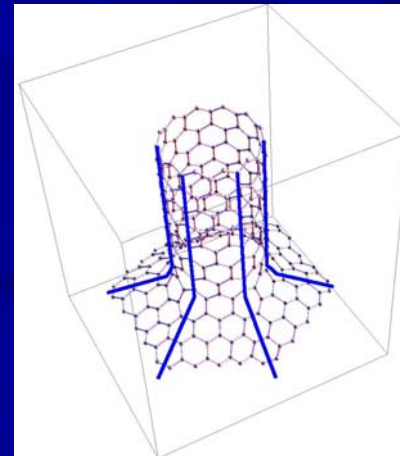
(48,0)



(from J. G., F. Guinea and J. Herrero, Phys. Rev. B 79, 165434 (2009))

The local DOS is shown here in different sectors labelled by the eigenvalue for a  $\pi/3$  rotation,

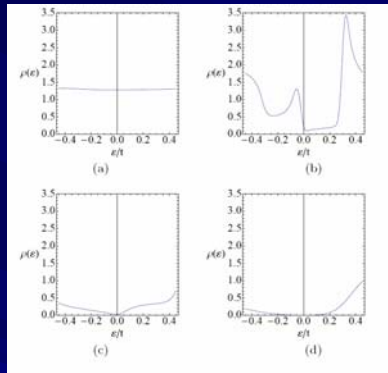
$q = 1$  (a),  $e^{\pm i\pi/3}$  (b),  $e^{\pm 2i\pi/3}$  (c),  $-1$  (d).



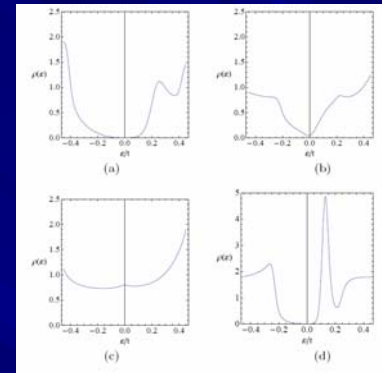
# CARBON NANOTUBE-GRAPHENE JUNCTIONS

It turns out that all the junctions fall into two different classes, depending on whether the nanotube geometry is  $(6n,0)$  with  $n$  a multiple of 3 or not.

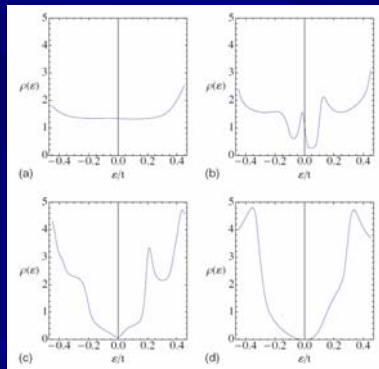
(18,0)



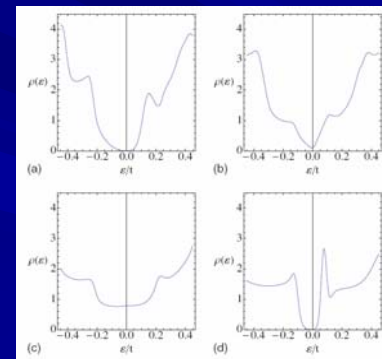
(24,0)



(54,0)



(48,0)



We observe that there is in general a depletion in the DOS at low energies, except in the sector  $q = 1$  when  $n$  is a multiple of 3, and the sector  $q = e^{\pm 2i\pi/3}$  when  $n$  is not a multiple of 3, which is related to the fact that the branches with lowest energy of zig-zag carbon nanotubes have a nonvanishing angular momentum  $\pm 4n$ .

# CARBON NANOTUBE-GRAPHENE JUNCTIONS

Within each class, all the DOS look very similar, even for different geometries of the nanotube, with the position of the main features scaled in inverse proportion to the radius  $R$  of the tube.

This leads to think that there may exist a unified description in terms of the Dirac equation in the curved space

$$iv_F \boldsymbol{\sigma} \cdot (\nabla \mp ie\mathbf{A}) \Psi^\pm = \varepsilon \Psi^\pm$$

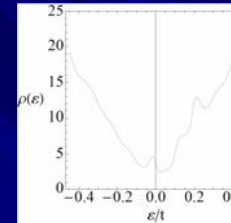
$$iv_F \left( \partial_r + \frac{i\partial_\theta}{r} \pm \frac{\Phi}{r} + \frac{1}{2r} \right) \Psi_A^\pm(r, \theta) = \varepsilon \Psi_B^\pm(r, \theta)$$

$$iv_F \left( \partial_r - \frac{i\partial_\theta}{r} \mp \frac{\Phi}{r} + \frac{1}{2r} \right) \Psi_B^\pm(r, \theta) = \varepsilon \Psi_A^\pm(r, \theta)$$

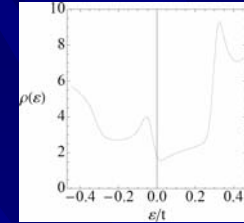
$$iv_F \left( \partial_z + \frac{i\partial_\theta}{R_0} \right) \Psi_A^\pm(z, \theta) = \varepsilon \Psi_B^\pm(z, \theta)$$

$$iv_F \left( \partial_z - \frac{i\partial_\theta}{R_0} \right) \Psi_B^\pm(z, \theta) = \varepsilon \Psi_A^\pm(z, \theta)$$

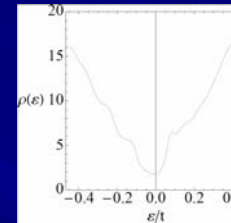
(54,0)



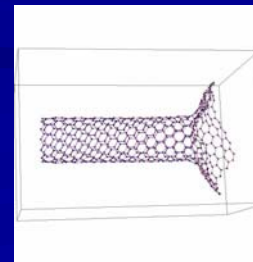
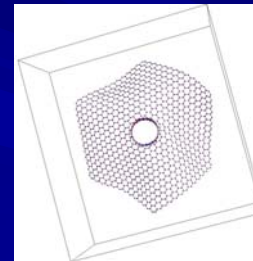
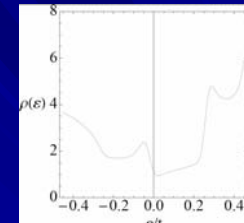
(18,0)



(48,0)

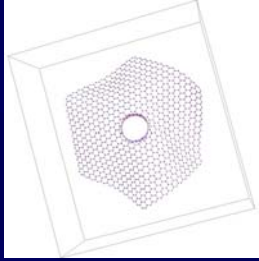


(12,12)

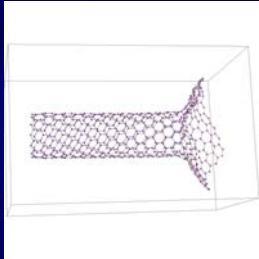


# CARBON NANOTUBE-GRAPHENE JUNCTIONS

The solutions in each side of the junction are



$$\begin{pmatrix} \Psi_A^\pm(r, \theta) \\ \Psi_B^\pm(r, \theta) \end{pmatrix} \equiv c_1 \begin{pmatrix} J_{n \mp \Phi - \frac{1}{2}}(pr) \\ -i \operatorname{sgn}(\varepsilon) J_{n \mp \Phi + \frac{1}{2}}(pr) \end{pmatrix} e^{in\theta} + c_2 \begin{pmatrix} Y_{n \mp \Phi - \frac{1}{2}}(pr) \\ -i \operatorname{sgn}(\varepsilon) Y_{n \mp \Phi + \frac{1}{2}}(pr) \end{pmatrix} e^{in\theta} \quad \varepsilon = \pm v_F p$$



$$\begin{pmatrix} \Psi_A^\pm(z, \theta) \\ \Psi_B^\pm(z, \theta) \end{pmatrix} \equiv \begin{cases} c'_1 \begin{pmatrix} 1 \\ -\operatorname{sgn}(\varepsilon) e^{i\phi(k)} \end{pmatrix} e^{ikz} e^{in\theta} + c'_2 \begin{pmatrix} 1 \\ \operatorname{sgn}(\varepsilon) e^{-i\phi(k)} \end{pmatrix} e^{-ikz} e^{in\theta} \\ c \begin{pmatrix} 1 \\ -\operatorname{sgn}(\varepsilon) e^{i\phi(-i\kappa)} \end{pmatrix} e^{\kappa z} e^{in\theta} \end{cases} \quad \varepsilon = \begin{cases} \pm v_F \sqrt{k^2 + \frac{n^2}{R_0^2}} & |\varepsilon| > \frac{v_F |n|}{R_0} \\ \pm v_F \sqrt{-\kappa^2 + \frac{n^2}{R_0^2}} & |\varepsilon| \leq \frac{v_F |n|}{R_0} \end{cases}$$

The nanotube-graphene junction can be viewed as an unconventional scattering potential, as electrons can be scattered off the layer into the nanotube. The scattering problem is solved by matching the wave functions at  $r = R_0$  and  $z = 0$ :

$$c_1 \begin{pmatrix} J_n(pR_0) \\ -i J_{n+1}(pR_0) \end{pmatrix} + c_2 \begin{pmatrix} Y_n(pR_0) \\ -i Y_{n+1}(pR_0) \end{pmatrix} = c'_2 \begin{pmatrix} 1 \\ e^{-i\phi(k)} \end{pmatrix}, \quad v_F p = v_F \sqrt{k^2 + \frac{n^2}{R_0^2}}$$

# CARBON NANOTUBE-GRAPHENE JUNCTIONS

$$c_1 \begin{pmatrix} J_n(pR_0) \\ -i J_{n+1}(pR_0) \end{pmatrix} + c_2 \begin{pmatrix} Y_n(pR_0) \\ -i Y_{n+1}(pR_0) \end{pmatrix} = c'_2 \begin{pmatrix} 1 \\ e^{-i\phi(k)} \end{pmatrix}, \quad v_F p = v_F \sqrt{k^2 + \frac{n^2}{R_0^2}}$$

We find an amplitude for transmission into the nanotube

$$T_n = \sqrt{\frac{\pi p R_0}{2}} \frac{i J_{n+1}(pR_0) Y_n(pR_0) - i J_n(pR_0) Y_{n+1}(pR_0)}{i Y_n(pR_0) - Y_{n+1}(pR_0) e^{i\phi(k)}}$$

This transmission is suppressed at low energies except for  $n = 0$ . At high energies,

$$\lim_{pR_0 \rightarrow \infty} T_n \approx \frac{i}{i \sin(pR_0 - \frac{n\pi}{2} - \frac{\pi}{4}) + \cos(pR_0 - \frac{n\pi}{2} - \frac{\pi}{4}) e^{i\phi(k)}} \rightarrow e^{i(pR_0 - \frac{n\pi}{2} - \frac{\pi}{4})}$$

This shows that

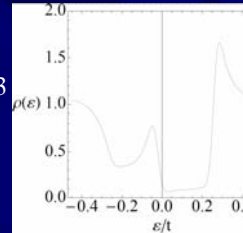
- low-energy electrons in the graphene layer, with  $\varepsilon < v_F / R_0$ , are scattered by the nanotube (except for angular momentum  $n = 0$ )
- high-energy electrons, with  $\varepsilon \gg v_F / R_0$ , have increasing probability of being transmitted into the nanotube
- at low energies and in the vicinity of the junction, there is in general a depletion of the density of states

# LOCALIZED STATES

What is then responsible for the peaks within the depleted DOS at very low energies?

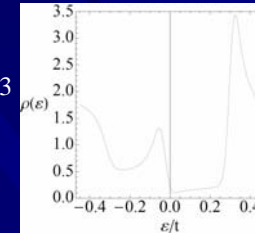
(12,12)

$$q = e^{\pm i\pi/3}$$



(18,0)

$$q = e^{\pm i\pi/3}$$



We may look for bound states of the Dirac equation, that can only take place at  $\epsilon = 0$

$$i \begin{pmatrix} 0 & \partial_r - \frac{1}{r} i \partial_\theta \mp \frac{\Phi}{2\pi r} + \frac{1}{2r} \\ \partial_r + \frac{1}{r} i \partial_\theta \pm \frac{\Phi}{2\pi r} + \frac{1}{2r} & 0 \end{pmatrix} \begin{pmatrix} \Psi_A^\pm \\ \Psi_B^\pm \end{pmatrix} = 0$$

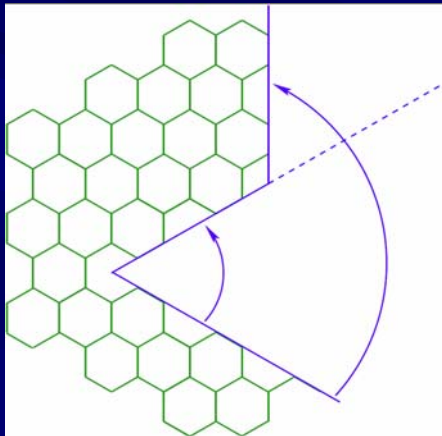
It is then possible to have localized states. Taking the maximum flux  $\Phi = 3\pi$ , we have for instance

$$\begin{aligned} \Psi_A^+ &\sim r^{n-\Phi/2\pi-1/2} e^{in\theta} & , \Psi_B^+ &= 0 & r > R_0 \\ \Psi_A^+ &\sim e^{n(z/R_0)} e^{in\theta} & , \Psi_B^+ &= 0 & z < 0 \end{aligned}$$

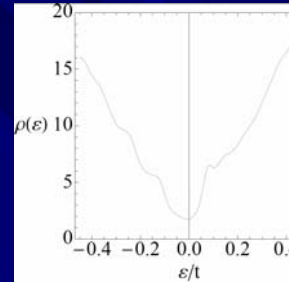
We find a state with  $n = 1$  which has an amplitude decaying in both the plane and the nanotube. Similarly, we have another localized state with  $n = -1$  in the other sublattice of the graphene layer. These localized states are then consistent with the above low-energy peak in the DOS.

# LOCALIZED STATES

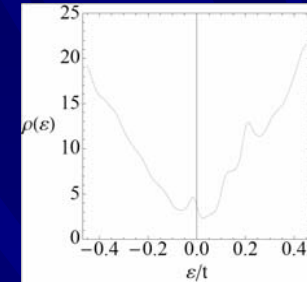
However, we know that the local DOS does not have in general a low-energy peak, except in junctions with armchair or  $(6n,0)$  nanotubes when  $n = 3p$



(48,0)



(54,0)



This different behavior is due to the fact the combined effect of the topological defects does not lead to the addition of the gauge flux (P. E. Lammert and V. H. Crespi, Phys. Rev. B 69, 035406 (2004))

$$R_{\pi/3} T(M,N) R_{\pi/3} = i\tau_2 e^{i(\pi/6)\sigma_z} e^{i(2\pi/3)(M-N)\tau_3} i\tau_2 e^{i(\pi/6)\sigma_z}$$

Thus, the effect of two heptagonal rings leads to  $\Phi = \pi$  when  $M-N$  is a multiple of 3, and to  $\Phi = \pi/3$  otherwise.

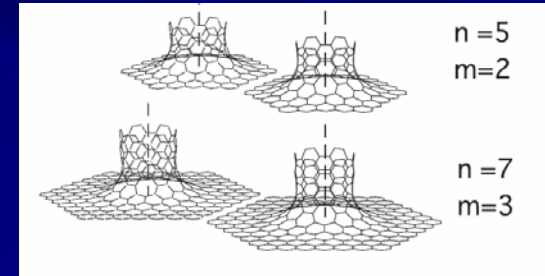
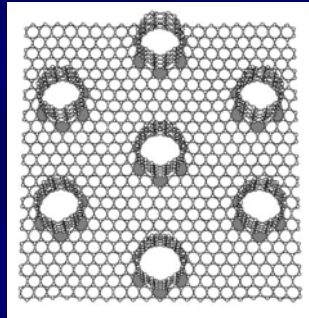
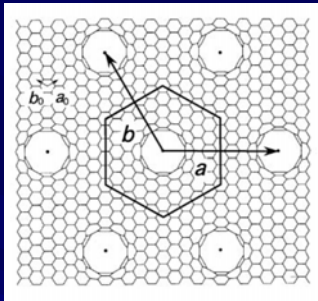
But a total flux of  $\Phi = \pi$  for the six heptagonal rings is not enough to localize states

$$\begin{aligned} \Psi_A^+ &\sim r^{n-\Phi/2\pi-1/2} e^{in\theta} & , \Psi_B^+ &= 0 & r > R_0 \\ \Psi_A^+ &\sim e^{n(z/R_0)} e^{in\theta} & , \Psi_B^+ &= 0 & z < 0 \end{aligned}$$

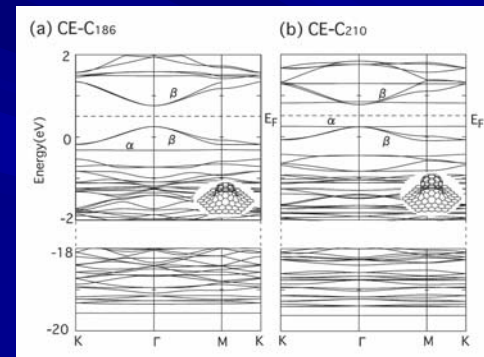
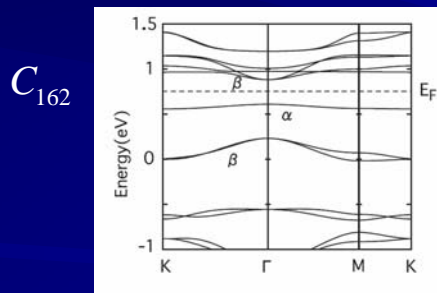
which explains the absence in general of low-energy peaks in the local DOS at the junction.

# ARRAYS OF NANOTUBE-GRAPHENE JUNCTIONS

The arrays of nanotube-graphene junctions have been studied before in the case of short armchair nanotubes by T. Matsumoto and S. Saito, *J. Phys. Soc. Japan* **71**, 2765 (2002):



The most important findings were the semiconducting behavior of the undoped system, and the appearance of very flat bands at low energies



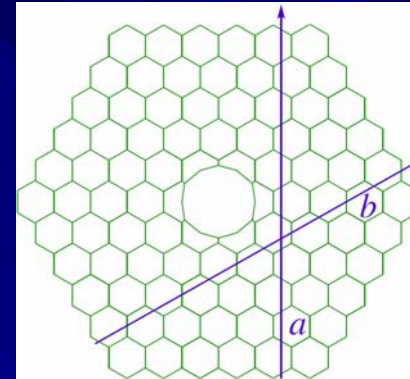
(from T. Matsumoto and S. Saito, *J. Phys. Soc. Japan* **71**, 2765 (2002))

One may ask what would be the electronic structure of junctions with much longer nanotubes, and the dependence on their geometry.

# ARRAYS OF NANOTUBE-GRAPHENE JUNCTIONS

A convenient computational approach is to consider a hexagonal patch around one of the junctions as unit cell of the material.

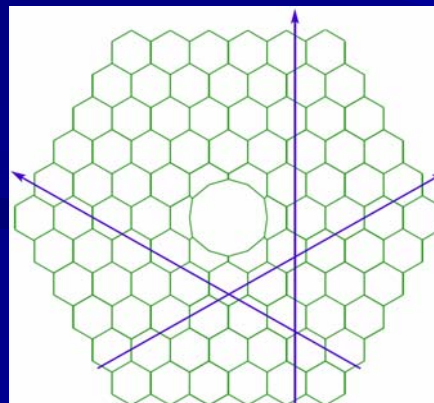
The Brillouin zone for this superlattice is an hexagon, with size inversely proportional to the distance  $L$  between the junctions. We can find all the subbands by looking for eigenstates within this unit cell with appropriate boundary conditions.



Thus, for a state with momentum  $k$ , we just have to diagonalize a tight-binding hamiltonian matching opposite boundaries of the unit cell with the phase factors

$$e^{ik \cdot \mathbf{a}} = e^{ik_y L}$$

$$e^{ik \cdot (\mathbf{a}-\mathbf{b})} = e^{i(-\sqrt{3} k_x/2 + k_y/2)L}$$



$$e^{ik \cdot \mathbf{b}} = e^{i(\sqrt{3} k_x/2 + k_y/2)L}$$

# ARRAYS OF NANOTUBE-GRAPHENE JUNCTIONS

As in the case of the individual junctions, we may classify the different arrays by the geometry of their nanotubes.

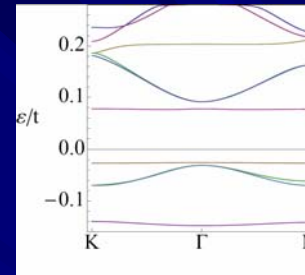
One of the classes is constituted by the arrays with armchair or  $(6n,0)$  nanotubes for which  $n$  is a multiple of 3. This is characterized by presence of a series of very flat bands that may become close to the Fermi level.

The other class comprises the junctions with the rest of nanotubes and corresponds to the case where all the bands are dispersive.

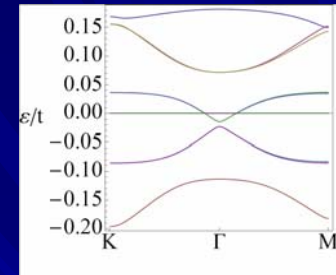
As a general rule:

- the dispersive bands are shifted towards the Fermi level as the distance between the junctions in the array is enlarged
- the number of flat bands grows at low energies as the nanotube length is increased, reflecting that their origin lies in the existence of states confined within the nanotubes

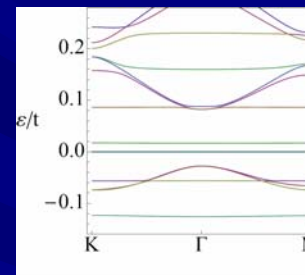
(12,12)



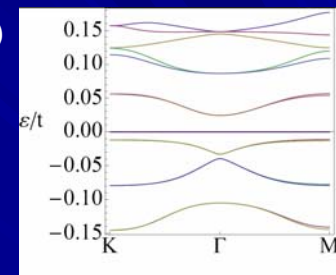
(12,0)



(18,0)



(24,0)



To summarize,

carbon-nanotube junctions offer the possibility to observe interesting electronic properties:

- they show the ubiquity of the Dirac equation in the description of carbon materials
- they have states that propagate through the junction, localized states, and states confined to the nanotube side
- they lead to remarkable electronic structure in the case of arrays of nanotube-graphene junctions